Postprint of: Wagner-Wysiecka E., Szarmach M., Chojnacki J., Łukasik N., Luboch E., Cation sensing by diphenyl-azobenzocrowns, Journal of Photochemistry and Photobiology A: Chemistry, Vol. 333 (2017), pp. 220-232, DOI: 10.1016/j.jphotochem.2016.10.028

CATION SENSING BY DIPHENYL-AZOBENZOCROWNS

Ewa Wagner-Wysiecka[a,*], Mirosław Szarmach[a], Jarosław Chojnacki[b], Natalia Łukasik[a], Elzbieta Luboch[a,*]

[a] Department of Chemistry and Technology of Functional Materials, Gdansk University of Technology, Narutowicza 11/12, 80-233 Gdansk, Poland [b] Department of Inorganic Chemistry, Faculty of Chemistry, Gdansk University of Technology, Narutowicza 11/12, 80-233 Gdansk, Poland
* Corresponding authors
E-mail addresses:
ewa.wagner-wysiecka@pg.gda.pl (E. Wagner-Wysiecka), elzbieta.luboch@pg.gda.pl (E. Luboch)

Abstract
Metal cations complexation and proton binding by 13- and 16-membered diphenyl-azobenzocrowns and diphenyl-hydroxyazobenzocrowns were studied in acetonitrile using spectroscopic methods: UV–vis spectroscopy, spectrofluorimetry, and ^{1}H NMR spectroscopy. Phenyl moieties in benzene rings were found to affect binding strength alkali and alkaline earth metal cations and hydrogen ion, and affect tautomeric equilibrium of hydroxyazobenzocrowns. X-ray structure of 13-membered diphenylhydroxyazobenzocrown was solved showing the existence of this compound in quinone-hydrazone form in a solid state. The suitability of diphenyl-azobenzocrowns for potentiometric metal cation determination using miniature, planar, all-solid-state type electrodes was also tested.

Keywords: Azobenzocrowns, Metal cation complexation, UV-vis spectroscopy, Fluorescence, Ion-selective electrodes

1. Introduction

Azobenzene moiety, well known since more than 100 years (*trans* azobenzene was first described in 1834), due to its photo and redox activity, is still one of the most common chromophore inserted as a part of more sophisticated chemical structures [1]. Well known phenomena for substituted azobenzenes bearing hydroxy group in *para* position to azo moiety (but also aminoazocompounds) is azophenol – quinone-hydrazone tautomerism [2]. Because of different optical and physical properties of tautomers these systems are interesting objects of studies not only from academic but also practical point of view [3]. A curious group of azocompounds are crown ethers azobenzocrowns in which 2,2'-substituted azobenzene residue is an inherent part of a macrocycle. The simplest 13- and 16-membered azobenzocrowns **A** and **B** are shown in Fig. 1 [4]. Within more than 20 years, a numerous derivatives of azobenzocrowns of different size of macrocycle and diverse type of substituents in benzene rings were prepared and studied as e.g.: ionophores in membrane ion-selective electrodes (ISEs), components of electroactive and photoactive monolayers and chromoionophores [5]. 13- and 16- membered azobenzocrowns **1** and **2** were previously used as ionophores in classic membrane ion selective electrodes and furthermore compound **1** in ChemFETs (Chemically Modified Field Effect Transistors) [6,7]. Lipophilic compounds **1** and **2** are good ionophores for membrane ion selective electrodes. Typically for this class of compounds is sodium or potassium selectivity of sensors depending on the size of the macrocyclic cavity of ionophore. Recently, a considerable technological development in manufacturing of potentiometric sensors has been made. Nowadays, one of the trend is the preparation of miniature ion-selective sensors *all-solid-state* type [8]. Such sensors can be successfully used for the construction of integrated analytical platforms e.g. for clinical or environmental analysis [9]. But it is worth to note that not every ionophore suitable for classic ISEs works well in miniature, planar *all-solid-state* type electrodes. For example, compounds **A** and **B** are for this purpose insufficiently lipophilic. More lipophilic azobenzocrowns with hydrocarbon

https://doi.org/10.1016/j.jphotochem.2016.10.028

residues in para position to ether linkage were not studied as ionophores in membrane *all-solid-state* type electrodes up to now.

Azobenzene itself is hardly fluorescent [10] but there are some cases when fluorescence of azocompounds is measurable. There are several examples of fluorescent azocompounds functionalized with fluorophores, sterically hindered azocompounds and others [11]. In our previous papers we demonstrated that protonated forms of azobenzocrowns are fluorescent [12a] and the functionalization of macrocyclic azocompounds can lead to fluorescent metal cation probes [13]. Hydroxyazocompounds, for which the tautomeric equilibrium with the quinone-hydrazone form is stabilized by intramolecular hydrogen bond, are another example of fluorescent azocompounds [14]. Among other, the fluorescence of phenylazonaphthols was studied by Fischer [15] and Antonov[16], and phenylazopyrazolones were investigated by Polansky [17].

It was shown that the quinone-hydrazone form of hydroxyazocompounds is responsible for fluorescence. In this regard, macrocyclic hydroxyazobenzocrowns can be considered as analogs of aromatic hydroxyazocompounds.

Our last interest in azobenzocrowns chemistry is focused on hydroxyazobenzocrowns and studies of the relationship between tautomeric equilibrium and ion binding properties [6f, 12].

Here, we present new results on binding and ionophoric properties of 13- and 16-membered diphenyl-azobenzocrowns **1– 4** (Fig. 1). Synthetic procedures for studied compounds were elaborated and described earlier by us [6c, 7, 12b]. The crystal structure of quinone-hydrazone form of **3** is also presented.

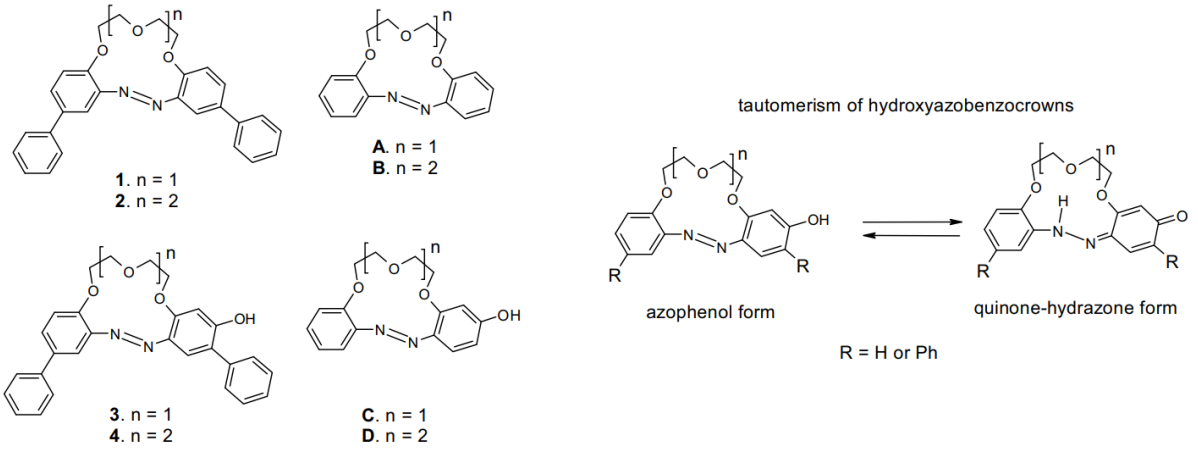

Fig. 1. Azobenzocrows **1-4** studied in this work, reference compounds **A-D** and tautomerism of hydroxyazobenzocrowns.

2. Results and discussion

2.1. Diphenyl-azobenzocrowns 1 and 2 metal cations complexation in solution and ionophoric properties in all-solid state electrodes

Azobenzocrown ethers form complexes with alkali and alkaline earth metal cations [4, 6d–f, 12]. Binding strength and selectivity of this process is dependent not only on macrocycle size but also on the type of substituents present in azocrown benzene rings. Relatively large and rigid phenyl rings in para position in relation to polyether linkage in azobenzocrowns **1–4** structure should also affect their ion affinity. Chromogenic character of azobenzocrowns allows the use of simple UV–vis spectroscopy to study ion-crown interaction. This method was used as the first for comparative binding studies of **1–4** and reference macrocycles **A–D**.

13-Membered azobenzocrowns selectively bind lithium cation among alkali metal cations in acetonitrile solution [4,6d]. Larger, 16-membered crowns form complexes both with alkali and alkaline earth metal ions [4c]. Previously [6d–f] it was shown, that the stability constant values of

https://doi.org/10.1016/j.jphotochem.2016.10.028

1:1 metal cation complexes of azobenzocrowns and the observed spectral shift of the complex band depend on the presence and nature of functional groups in benzene rings.

As it could be predicted the selective lithium complexation in acetonitrile was also found for 13-membered diphenyl-azobenzocrown ether **1**. Spectral changes observed upon titration of azobenzocrown **1** solution with lithium perchlorate in acetonitrile (Fig. 2) are comparable in trend (i.e. increase of intensity without a spectral shift) to changes observed for parent azobenzocrown **A** [4b]. Stability constant value of lithium complex logK 2.8 ± 0.1 is significantly lower for diphenyl derivative than for unsubstituted macrocycle **A** (logK 4.1) [4]. The presence of sodium and potassium salts did not affect absorption spectra at all.

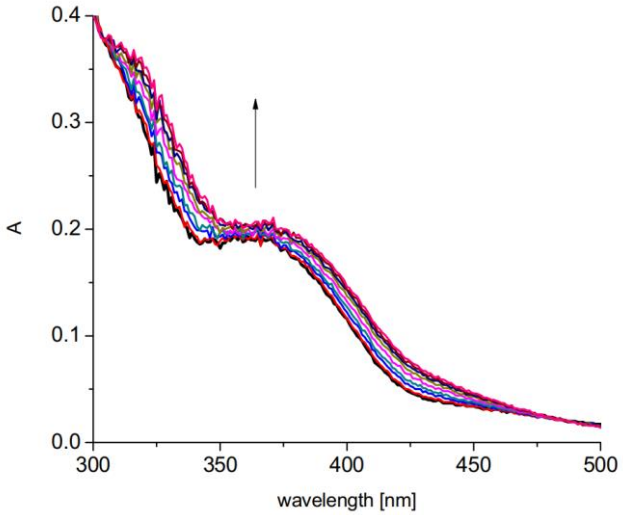

Fig. 2. Changes in UV-vis spectrum of **1** (4.2×10^{-5} M) upon titration with lithium perchlorate ($0\text{-}1.0 \times 10^{-3}$ M) in acetonitrile.

Comparison of stability constants (logK) for metal cation complexes of 16-membered crowns **2** and **B** (Fig. 3) shows no relevant difference in binding strength of lithium and sodium cations. However, opposite to crown **B** no spectral changes were found for **2** in the presence of potassium perchlorate. Interesting and different than for **B** is the trend of stability constant values for alkaline earth metal cations complexes. For diphenyl derivative **2** the increase of stability constant values is in agreement with the increase of ion diameter: the smallest value of stablility constant was found for magnesium and the largest for barium complex. Binding strength for **2** is almost in reverse order to **B** complexes [4].

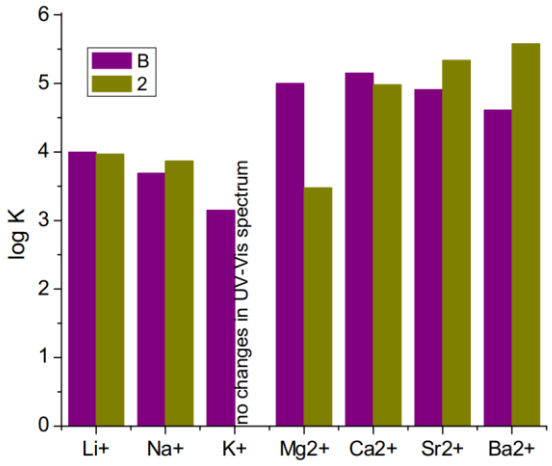

Fig. 3. Comparison of stability constant values (logK) of complexes (1:1) of **B** [4] and **2** with metal perchlorates in acetonitrile.

https://doi.org/10.1016/j.jphotochem.2016.10.028

The above studies show pronounced differences in binding strength of metal cation by non-functionalized crowns **A** and **B** and their analogs with phenyl rings **1** and **2**. The presence of phenyl substituents affecting the size and shape of the molecular cavity (steric hindrance) can be an explanation of this. The selectivity and strength of host-guest interactions strongly depend on the environment, i.e. the solvent. The ionophoric properties of azobenzocrowns are different in polar acetonitrile and in ISEs where analytical signal is generated upon contact of the ionophore entrapped in non-polar environment (plasticizer and polymer matrix) with aqueous solution of salt.

Azobenzocrowns **1** and **2** were used as potential sodium or potassium ionophores in miniature graphite (screen-printed) membrane ion-selective electrodes. Besides the ionophore, the components of membrane were: PVC, *o*-nitrophenyl-octyl ether (*o*-NPOE), potassium *tetrakis*(4-chlorophenyl)borate and carbon nanotubes. As an example, potassium and sodium responses of screen-printed graphite electrode with membrane doped with 16-membered diphenyl-azobenzocrown **2** are shown in Fig. 4.

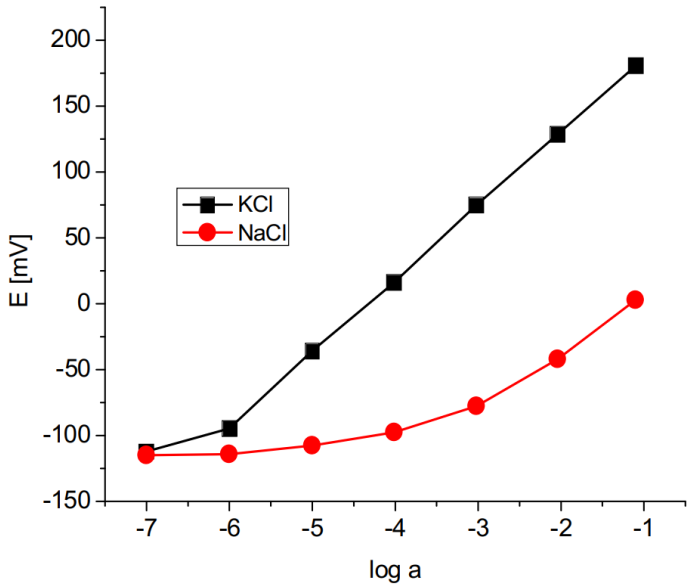

Fig. 4. Sodium and potassium responses of graphite screen-printed electrodes with membrane containing 16-membered diphenyl-azobenzocrown **2** as ionophore.

Table 1 lists the parameters of selected screen printed electrodes based on the compounds **1** and **2**. The values of potentiometric selectivity coefficients (log$K_{Na/X}$ and log$K_{K/X}$) for sodium and potassium selective screen printed electrodes are also illustrated in Fig. 5.

Table 1. Characteristics and selectivity coefficients (SSM method, 10^{-1} M) of the graphite screen-printed ion-selective membrane electrodes based on compounds **1** and **2**.

Ionophore	Selective response towards…	Slope [mV/dec]	Lower detection limit log[a]	log$K_{Na/X}$ or log$K_{K/X}$							
				X:	K	Na	Li	Mg	Ca	NH_4	H
1	Na^+	61.1	-5.3		-2.5	-	-3.0	-4.9	-4.6	-2.8	-0.8
2	K^+	56.1	-6.4		-	-3.3	-4.1	-5.0	-4.5	-1.5	-3.0

The obtained selectivity coefficient [18] log$K_{Na,K}$ = -2.5 (SSM, 10^{-1} M) for miniature sodium selective electrode with 13-membered ionophore **1** is better than both for classic electrode and ChemFET [7]. Moreover, it is the best result (besides screen printed electrode with bisazobenzocrown described earlier [12b]) obtained for the whole group of the electrodes based on the 13-membered azobenzocrowns. Electrodes with compound **1** in membrane have better Na/K selectivity than electrodes with most commercial sodium ionophores [19].

https://doi.org/10.1016/j.jphotochem.2016.10.028

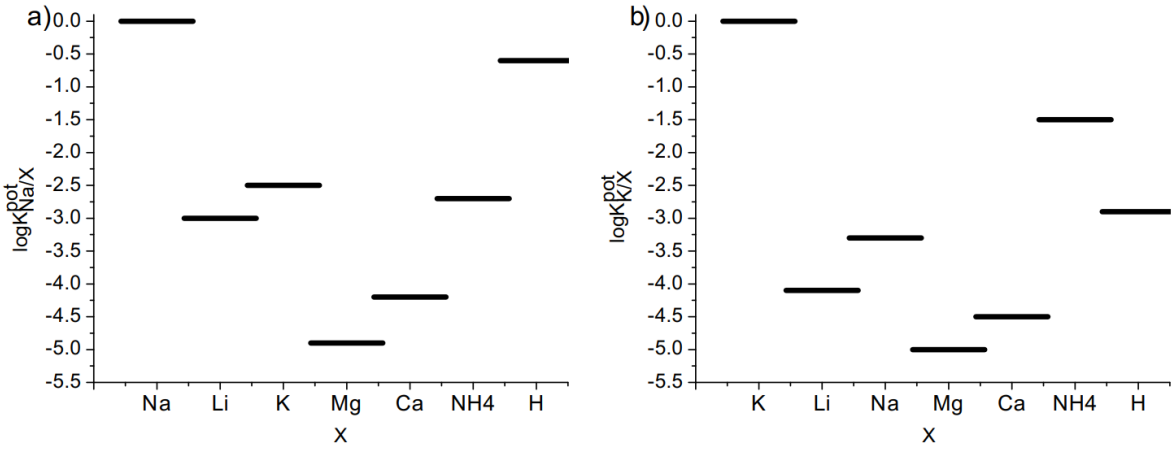

Fig. 5. Potentiometric selectivity coefficients ($\log K_{Na/X}$ and $\log K_{K/X}$) for a) sodium and b) potassium selective screen-printed electrodes with membranes doped azobenzocrown **1** and **2**.

Electrode with 16-membered macrocycle **2** as ionophore is potassium selective and the selectivity coefficient $\log K_{K,Na}$ = -3.3 (SSM, 10^{-1} M) is similar to that of classic electrode ([6c], here determined by another method (FIM)) but detection limit is improved.

Screen-printed electrode with **2** as ionophore is also less sensitive to pH ($\log K_{K,H}$ = -3.0) than classic sensor based on the same ion-carriers ($\log K_{K,H}$ = -0.7) [6c].

2.2. Diphenyl-hydroxyazobenzocrowns - tautomerism and metal cation complexation

Metal cation complexation can affect tautomeric equilibrium of macrocyclic host molecules [20]. Similar effect is also expected for azobenzocrowns **3** and **4** (Fig. 1) being analogs of macrocycles **C** and **D**. The presence of phenyl rings can influence the metal cation complexation as it was proved above for compounds **1** and **2**. On the other hand it can also affect azophenol-quinone-hydrazone tautomeric equilibrium. Metal cation complexation by hydroxyazobenzocrowns is strongly dependent on tautomeric equilibrium [6f,12]. Thus comparison of cation binding ability of functionalized macrocycles **3** and **4** with two phenyl moieties in meta position to azo group (*para* position to ether linkage) with unsubstituted in benzene rings hydroxyazobenzocrowns **C** and **D** seems to be worth of investigation.

2.2.1. ^{1}H NMR and UV–vis spectroscopy studies

^{1}H NMR spectra registered in various solvents show that compound **3** exists in acetonitrile in the quinone-hydrazone form. This is also the only tautomeric form in acetone [12b]. The quinone-hydrazone tautomer dominates in DMSO with phenolic form presence only in ~10%. In the case of **C** ~30% of azophenol form is observed under the same conditions [6d].

^{1}H NMR spectra of **3** registered in acetonitrile-d_3 and DMSO-d_6 are shown in Fig. 6. The most characteristic for quinone-hydrazone are signals of N-H proton and proton of quinone ring in *orto* position to ether linkage. The signals are observed as singlets at 12.67 and 5.95 ppm in acetonitrile and 12.64 and 6.07 ppm in DMSO. In DMSO-d_6 O-H and C-H proton signals characteristic for the azophenol form (shown in high amplification, Fig. 6 bottom): are observed at 10.56 and 6.76 ppm. Tautomeric forms have also different pattern and the position of ether proton signals (~4.4– 3.8 ppm). In the case of the quinone-hydrazone tautomer four signals of ether protons – one for each CH_2 group – are clearly differentiated. For azophenol tautomer two signals are observed.

The effect of tautomeric equilibrium on metal cation binding by **3** was investigated with the use of UV–vis and ^{1}H NMR spectroscopy.

https://doi.org/10.1016/j.jphotochem.2016.10.028

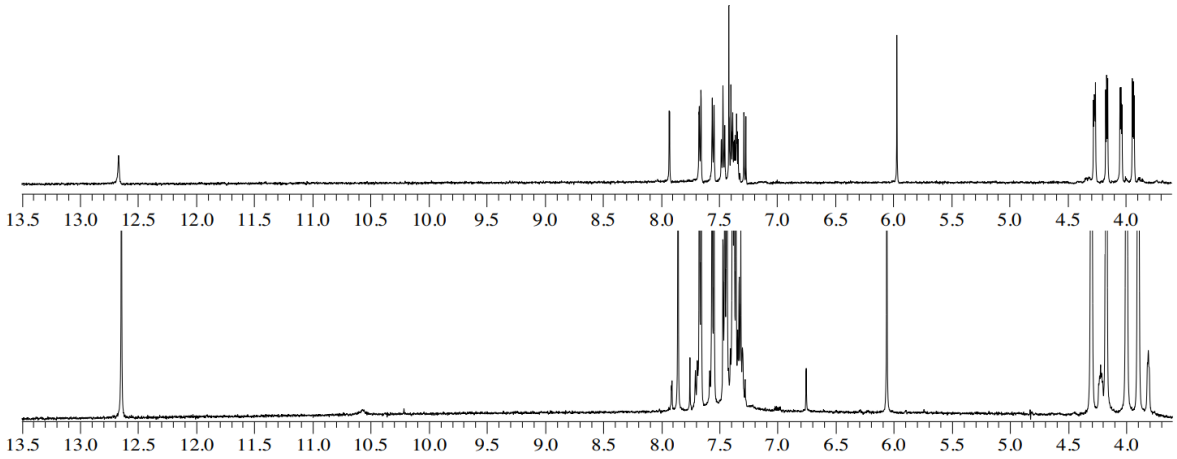

Fig. 6. ^{1}H NMR spectra of **3** in: top – acetonitrile-d_3 and bottom – DMSO-d_6 (high amplification).

Titration of **3** with lithium perchlorate in neutral acetonitrile causes small changes in absorption spectra (Fig. 7a), but in the presence of organic base – triethylamine – a noticeable (40 nm) shift of absorption band of complex and color change from yellow-orange to orange-red is observed (Fig. 7, top). From titration experiment in basic (Et_3N) acetonitrile the value of stability constant of lithium complex of 13-membered diphenyl-hydroxyazobenzocrown **3** was estimated as logK ~ 2.8. This value is slightly lower than for compound without phenyl rings **C** (logK ~3.2) [6d], but surprisingly almost the same as for diphenylazobenzocrown **1** (see above). Selective lithium complexation is in good agreement with the results obtained for series of 13-membered hydroxyazobenzocrowns where metal cation complexation was observed only in the presence of organic base [6][6f].

Sodium and potassium perchlorates used even in large excess (600-fold) in the presence of 240-fold excess of triethylamine do not affect strongly the absorption spectra of **3** (Fig. 7b). Addition to this solution of lithium perchlorate only in 6-fold excess in relation to **3** causes significant changes in absorption spectrum pointing reaction selectivity for lithium in the presence of large excess of sodium salt.

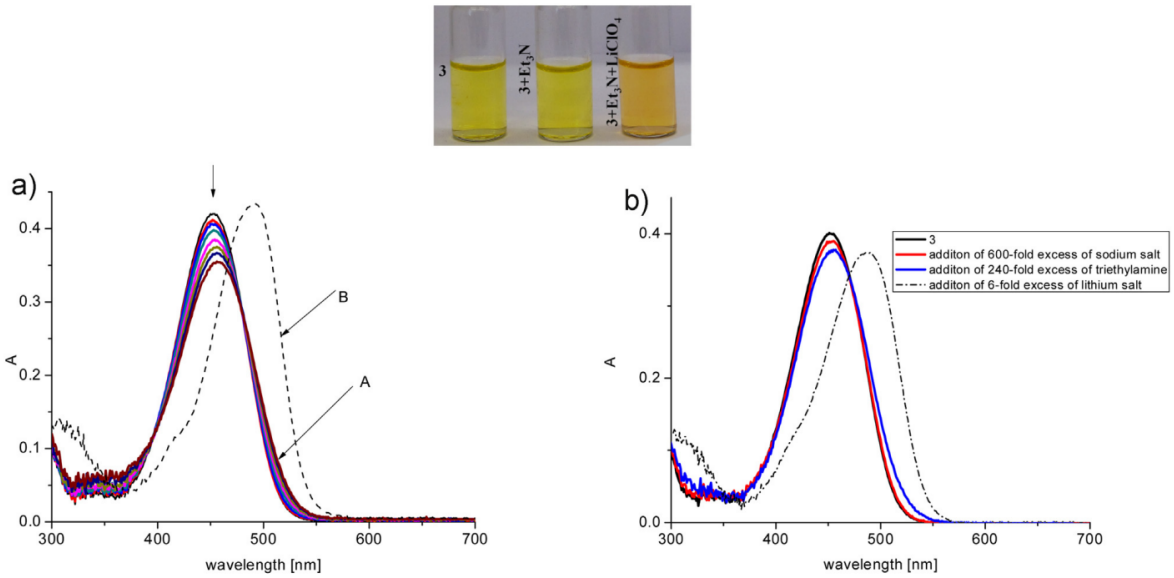

Fig. 7. Top: Comparison of color acetonitrile solution of **3** in the presence of triethylamine and lithium perchlorate. Bottom: a) UV-vis titration of **3** (7.2×10^{-5} M) with lithium perchlorate (0-5.5×10^{-2} M) in pure acetonitrile. Dashed line is spectrum registered upon addition to the titrated system solution of Et_3N (2.8×10^{-2} M); b) UV-vis spectra showing competitive binding of lithium by **3** in the presence of sodium salt and triethylamine in acetonitrile.

https://doi.org/10.1016/j.jphotochem.2016.10.028

No differences in ^{1}H NMR spectrum of **3** registered in neutral acetonitrile (Fig. 6 top) and spectrum registered in the presence of triethylamine (Fig. 8 top) were found. Addition to basic solution of **3** an excess of lithium perchlorate (Fig. 8 bottom) probably causes deprotonation of quinone-hydrazone form of **3** manifested in ^{1}H NMR spectrum among the others by disappearing the N-H signal and distribution polyether linkage proton signals. Thus it was assumed that disctinct spectral shift of absorption band is connected (similarly as for compound **C**) with complex formation by deprotonated quinone-hydrazone form of **3**.

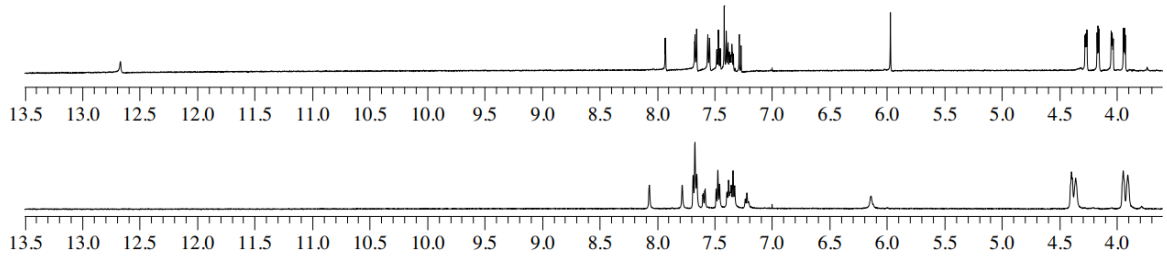

Fig. 8. Comparison of ^{1}H NMR spectra of **3** (1.6×10^{-3} M) registered in the presence of triethylamine (2.0×10^{-2} M; top) and both triethylamine and lithium perchlorate (3.9×10^{-2} M bottom) in acetonitrile-d_3 (spectra in high amplification because of low concentration of **3** and the excess of triethylamine).

Tautomeric equilibrium of 16-membered hydroxyazobenzocrowns is much more affected by the nature of the solvent than it is in the case of 13-membered analogs [6d]. It was stated [6e] that the higher macrocycle the higher the tendency of hydroxyazobenzocrown to exist in the azophenol form. It was found that in chloroform and acetonitrile crown **D** exists in the quinone-hydrazone form, but in highly dipolar DMSO it exists exclusively in the azophenol form. For azomacrocycle **4** – on the basis of analysis of H NMR spectra – the presence of quinone-hydrazone was found in chloroform and acetone [12b]. Although crowns **D** and **4** are hardly soluble in large concentrations in acetonitrile (10^{-2} M), what explains quality of presented spectra, the characteristic signals for quinone-hydrazone tautomers are observable (see Fig. 9a and e).

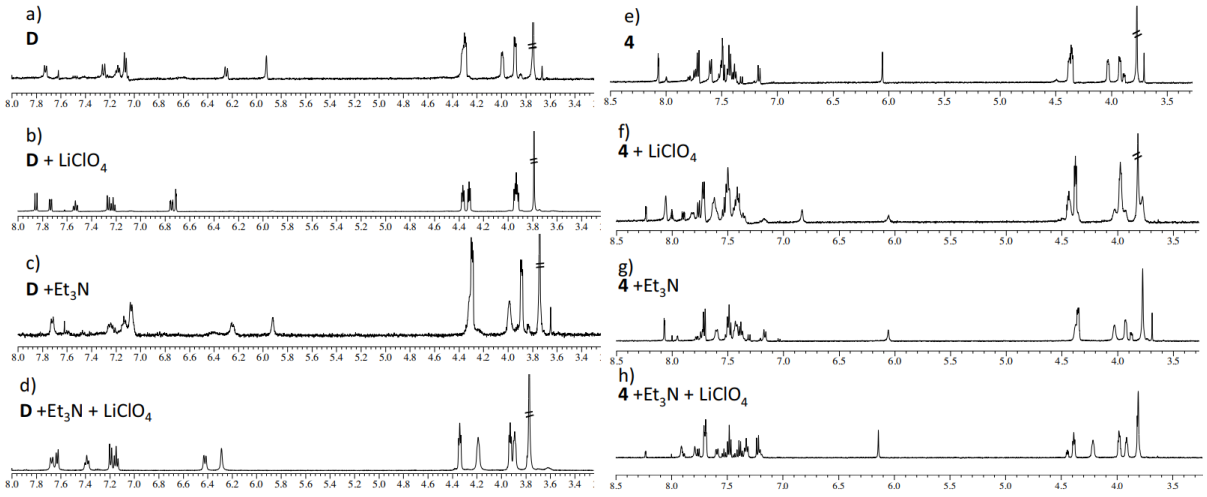

Fig. 9. Comparison of ^{1}H NMR spectra of 16-membered hydroxyazobenzocrowns **D** (left) and **4** (right) and spectra registered in the presence of lithium perchlorate; triethylamine and triethylamine and lithium perchlorate in acetonitrile-d_6.

Metal cation complexation by compound **D**, investigated by UV–vis spectroscopy, was signalized earlier [6d]. Opposite to 13-membered hydroxyazobenzocrown, blue shift for **D**

https://doi.org/10.1016/j.jphotochem.2016.10.028

was observed in the presence of lithium, sodium and alkaline earth metal (magnesium, calcium, strontium and barium) perchlorates in neutral acetonitrile. However, no changes in absorption spectra were observed upon titration of **4** with lithium and sodium perchlorates in neutral acetonitrile. It was stated, that metal cations are complexed by the azophenol form of **D**. This is supported by ^{1}H NMR spectrum of **D** (Fig. 9b) registered in the presence of lithium perchlorate, where the most characteristic signal of the quinone-hydazone form (~5.90 ppm) is not observed. In case of **4**, under the same conditions the mixture of the azophenol and quinone-hydrazone forms was observed (Fig. 9f).

Here, spectrophotometric metal cation complexation studies for **D** were widen to more detailed studies in basic (Et_3N) solution of acetonitrile, for comparison with the properties of 16-membered hydroxyazobenzocrown **4**.

Titration of **D** with lithium and sodium perchlorates in basic acetonitrile (Et_3N, pH ~10.5) results in an appearance of new, red-shifted band, exemplified here by changes in absorption spectra of **D** upon titration with lithium salt (Fig. 10a). Such spectral changes correspond well with data reported for 13-membered hydroxyazobenzocrowns where the quinone-hydrazone form was engaged in 1:1 complex formation [6f]. Potassium perchlorate does not cause spectral changes. Similar results were obtained for titration of **4** with lithium and sodium perchlorates. As examples spectral changes upon titration of **4** with lithium perchlorate in basic acetonitrile are shown in Fig. 10b. The determination of reliable stability constant of complexes **4** with alkaline earth metal cations was not possible under titration conditions. Although addition of magnesium, calcium, strontium and barium perchlorates to basic (Et_3N) acetonitrile solution of **4** results in appearance of a new band (red-shift), suggesting complex formation, systems returns to uncomplexed form of crown within experiment timescale. Stability constants values (logK) determined from UV–vis titrations of lithium and sodium complexes of **D** in neutral and basic acetonitrile and **4** in basic acetonitrile are shown in Fig. 10c. Additionally, stability constant of **B** was included in result set, having in mind that binding constant with lithium and sodium refers in this case to values found in neutral acetonitrile.

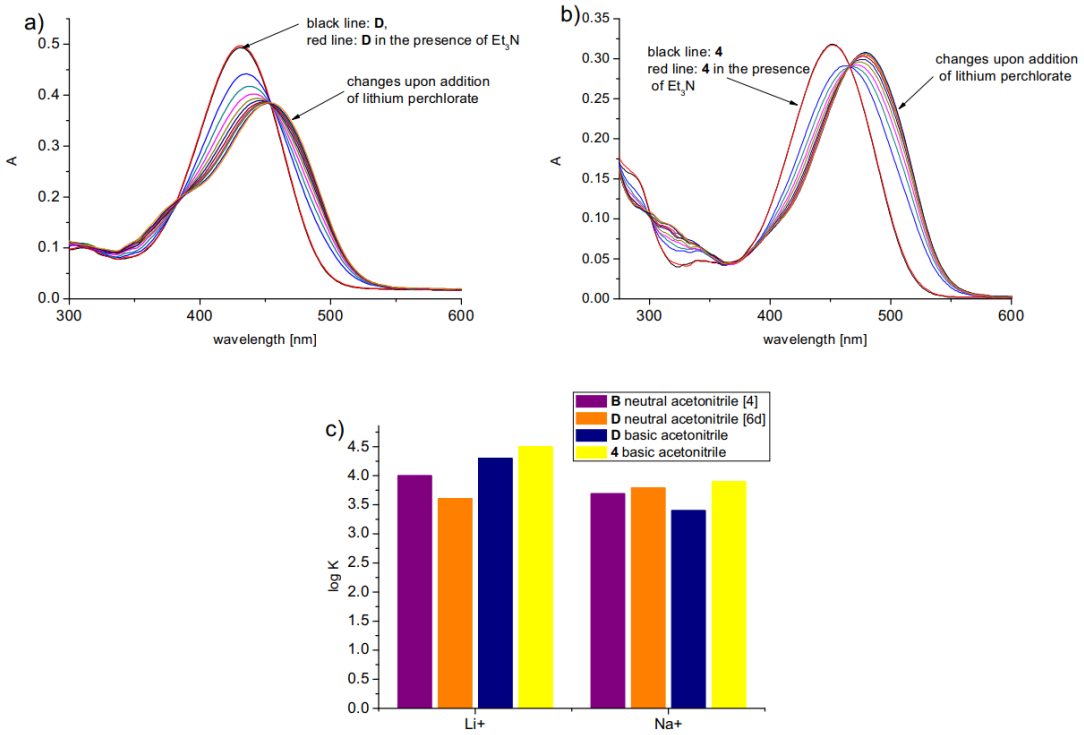

Fig. 10. Spectral changes upon titration of: a) **D** (3.0×10^{-5} M) with lithium perchlorate (0-3.5×10^{-4} M) in acetonitrile in the presence of triethylamine (pH ~10.5); b) **4** (3.7×10^{-5} M) with lithium perchlorate (0-3.2×10^{-5} M) in acetonitrile in the presence of triethylamine (pH ~10.5); c) comparison of stability constant values of complexes of **B** in neutral acetonitrile [4], **4** in basic acetonitrile [6d] and **D** both in neutral and basic acetonitrile calculated from UV-vis titrations.

https://doi.org/10.1016/j.jphotochem.2016.10.028

Lithium binding by 16-membered azobenzocrowns is stronger when complex is formed by the ionized quinone-hydrazone form (**D** and **4** in basic acetonitrile) than in complex in which the azophenol tautomer is engaged (**D** in neutral acetonitrile). It points that the quinone-hydrazone tautomer – probably ionized – has higher affinity to lithium cation than the azophenol form. The affinity to lithium in the latter case is even smaller than for non-fuctionalized crown **B**. Stability constant value for sodium complex is the highest for crown **4** in basic acetonitrile. Much more comparable are binding constants of sodium complexes of **B** and **D** in neutral acetonitrile. For 16-membered hydroxyazobenzocrowns the presence of phenyl rings appears to be major factor influencing tautomeric equilibrium driven by metal cation complexation and consequently the strength of ion-macrocyle interactions. Phenyl rings, as residue in *ortho* position to OH group, seem to stabilize the quinone-hydrazone form even in the presence of metal cations. It is well seen when comparing ^{1}H NMR of **D** and **4** registered in the presence of lithium perchlorate in neutral acetonitrile (Fig. 9b and Fig. 9f). In spectrum of **4**, besides the azophenol tautomer, signals of protons of the quinone-hydrazone form (~6 ppm) are observable. In the presence of triethylamine both crowns **D** and **4** form complexes with lithium in quinone-hydrazone form (Fig. 9d 1 and Fig. 9h). For comparison ^{1}H NMR spectra of **D** and **4** in basic (Et_3N) acetonitrile were shown in Fig. 9c and Fig. 9g.

2.2.2. Spectrofluorescence studies

For investigated here 13-membered hydroxyazobenzocrown **3** the quinone-hydrazone tautomer is the only form in acetonitrile. Its emission band is well observable at 560 nm (excitation wavelength 450nm) (Fig. 11a). Titration of **3** with lithium and sodium perchlorates in neutral acetonitrile causes slight decrease of fluorescence intensity. However, in the presence of trimethylamine lithium perchlorate fluorescence intensity of **3** strongly decreases (Fig 11a – dashed line). Stability constant of complex of **3** with lithium cation under spectrofluorimetric titration was estimated as logK ~2.4, what is slightly lower, but comparable to value obtained from UV-vis experiment. Fig. S1 (Supplementary data) shows an example of plot of $F_0/(F_0\text{-}F)$ versus 1/lithium perchlorate concentration used for evaluation of stability constant value of lithium complex of **3** from spectrofluorimetric measurements. Additionally, to evaluate the effect of the presence of lithium, sodium and organic base on fluorescence intensity of **3** Stern-Volmer constants (K_{SV}) were estimated and compared (Fig 11c). For **3**-lithium salt-Et_3N system K_{SV} is over 220 whereas for **3**-sodium perchlorate and trimethylamine it does not exceed 20. Relatively high K_{SV} value obtained for tetra-*n*-butylammonium perchlorate – used here to check the effect of a counter ion on fluorescence changes – can be attributed to fluorescence quenching by large and heavy tetra-*n*-butyl and perchlorate ions. Lithium driven fluorescence quenching in basic acetonitrile was also observed in the presence of large excess of sodium perchlorate (970-fold excess, Fig 11b) what in connection with results obtained from UV-vis experiments confirms high selectivity of lithium complexation over sodium cation. This process is selective for lithium system, because sodium salt used in large excess even in strongly basic solution (100-fold excess of trimethylamine) does not affect fluorescence spectrum in a such degree (Fig. 11b) as lithium cation. This selectivity can be explained by discrimination of metal cations according to their size and host-guest complementarity. Examples of Stern-Volmer plots for **3** are shown in Fig. S2a and S2b (Supplementary data). Quenching of fluorescence by lithium cation was also observed in basic acetonitrile for compound **C**, but in this case Stern-Volmer constant value was about 2.8-fold (K_{SV}~ 80) lower.

As the ionized quinone-hydrazone form of hydroxyazocompounds are not fluorescent, on the basis of above experiments we can state that lithium cation promotes deprotonation of the quinone-hydrazone form of hydroxyazobenzocrown **3**. This is supported by ^{1}H NMR spectra shown in Fig. 8.

Analogous experiments were carried out for 16-membered hydroxyazobenzocrowns **D** and **4**.

Titrations with alkali metal perchlorates were carried out both in neutral and in basic acetonitrile. Similarly to 13-membered crowns decrease of the intensity of the emission was observed upon addition of metal salts. As examples in Fig. 12a–d changes of fluorescence intensity of **D** and **4** upon titration with lithium perchlorate in neutral and in basic acetonitrile are compared.

https://doi.org/10.1016/j.jphotochem.2016.10.028

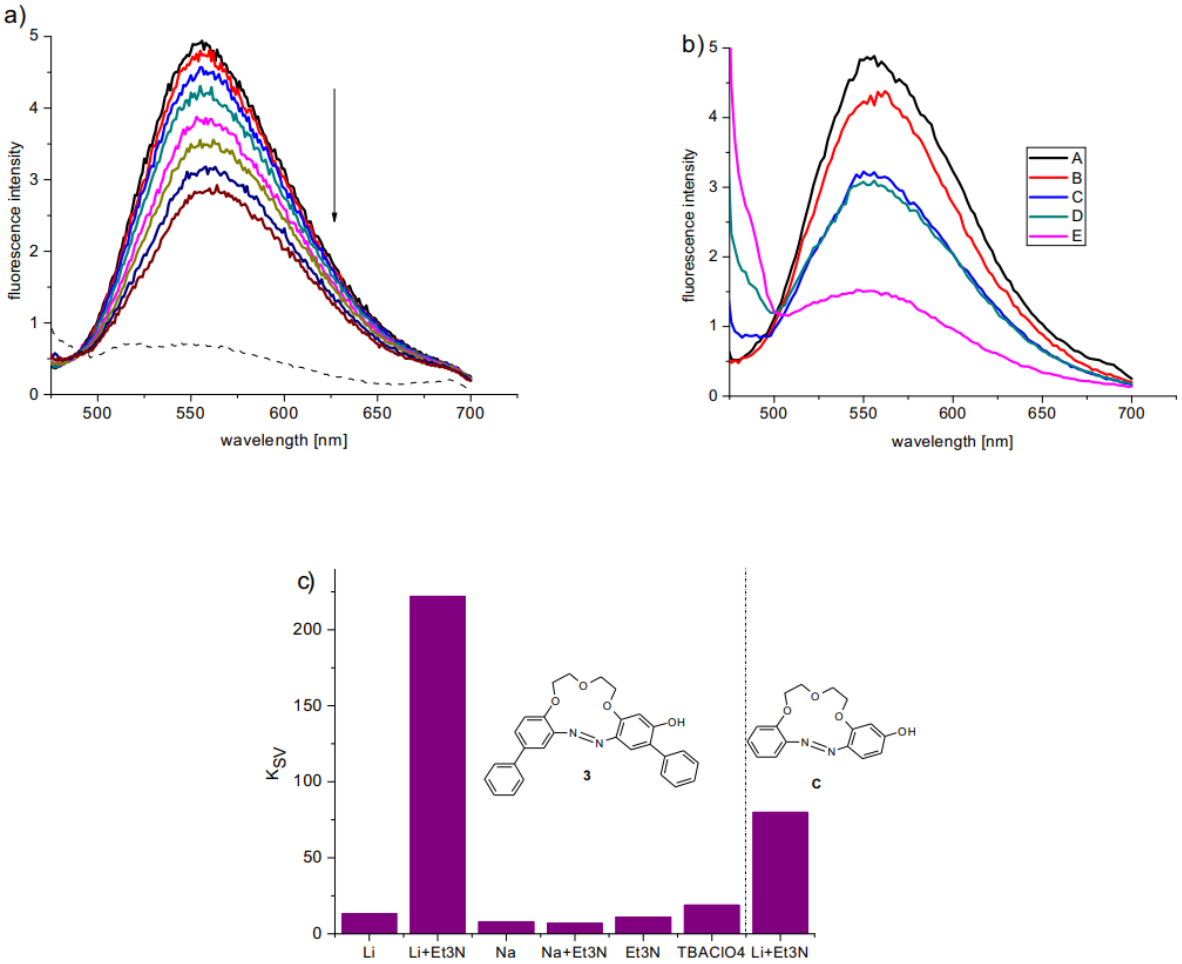

Fig. 11. Comparison of: a) fluorescence (λ_{ex} = 450 nm, λ_{em} = 560 nm) titration of **3** (7.2 × 10^{-5} M) with lithium perchlorate (0-5.5 × 10^{-2} M) in pure acetonitrile. Dashed line: spectrum registered upon addition to the titrated system of solution of Et_3N (2.8 × 10^{-2} M); b) fluorescence spectra showing competitive binding of lithium by **3** in the presence of sodium salt and triethylamine in acetonitrile. The spectra are registered upon subsequent addition to a measurement cell the respective solutions labeled as follows: A – **3** (7.2 × 10^{-5} M), B – 24-fold excess of triethylamine; C – 33-fold excess of triethylamine and 970-fold excess of sodium perchlorate; D - another portion of triethylamine: 40-fold excess; E – 97-fold excess of lithium perchlorate; c) The comparison of Stern-Volmer constant values for **3** (7.2 × 10^{-5} M) in acetonitrile (430-fold excess of triethylamine was used in titration experiments with lithium and sodium perchlorates). For comparison K_{SV} value determined for **C** system including lithium salt under the same conditions is shown.

Stern-Volmer constant values evaluated from titration experiments for **D** and **4** are collected in Fig. 13a and examples of Stern-Volmer plots (from single measurements) are shown in Fig. S3a and S3b (Supplementary data). It is worth to note again that, fluorescence quenching for **4** was observed both in neutral and in basic acetonitrile, whereas noticeable changes in absorption spectra were observed only in the presence of organic base. This is also valid for reported above 13-membered hydroxyazobenzocrowns. Collisional quenching of fluorescence probably is a dominating process in neutral acetonitrile for **3** and **4** whereas in case of **D** mixed dynamic and static quenching connected with formation of complex in ground state can be considered. Higher values of Stern-Volmer constants for 16-membered crown **D** than for diphenyl-hydroxyazobenzocrown **4** in neutral acetonitrile can be a result of these additive processes. In the presence of triethylamine where both the absorption and emission spectra of hydroxyazobenzocrowns are affected by metal cation presence, a decrease of fluorescence can be connected both with collisional quenching and complex formation by the ionized quinonehydrazone form. In this case higher values of Stern-Volmer constants were obtained

https://doi.org/10.1016/j.jphotochem.2016.10.028

for diphenyl-hydroxyazobenzocrown **4** preferentially complexing metal cations in the quinone-hydrazone form. Comparison of titration plots shown in Fig. 12a–d and fluorescence spectra of **4** registered in the presence of excess of tetra-*n*-butylammonium hydroxide (TBAOH) where a new band at 512 nm is observed (Fig. 13b) confirms that metal cation complexation process is connected with ionization of N-H bond of the quinone-hydrazone tautomers of diphenyl-hydroxyazobenzocrowns. Band corresponding to ionized quinonehydrazone form is also observable at 488 nm upon spectrofluorimetric titration of **D** with lithium and sodium perchlorates both in neutral and basic acetonitrile (Fig. 12a and Fig. 12c).

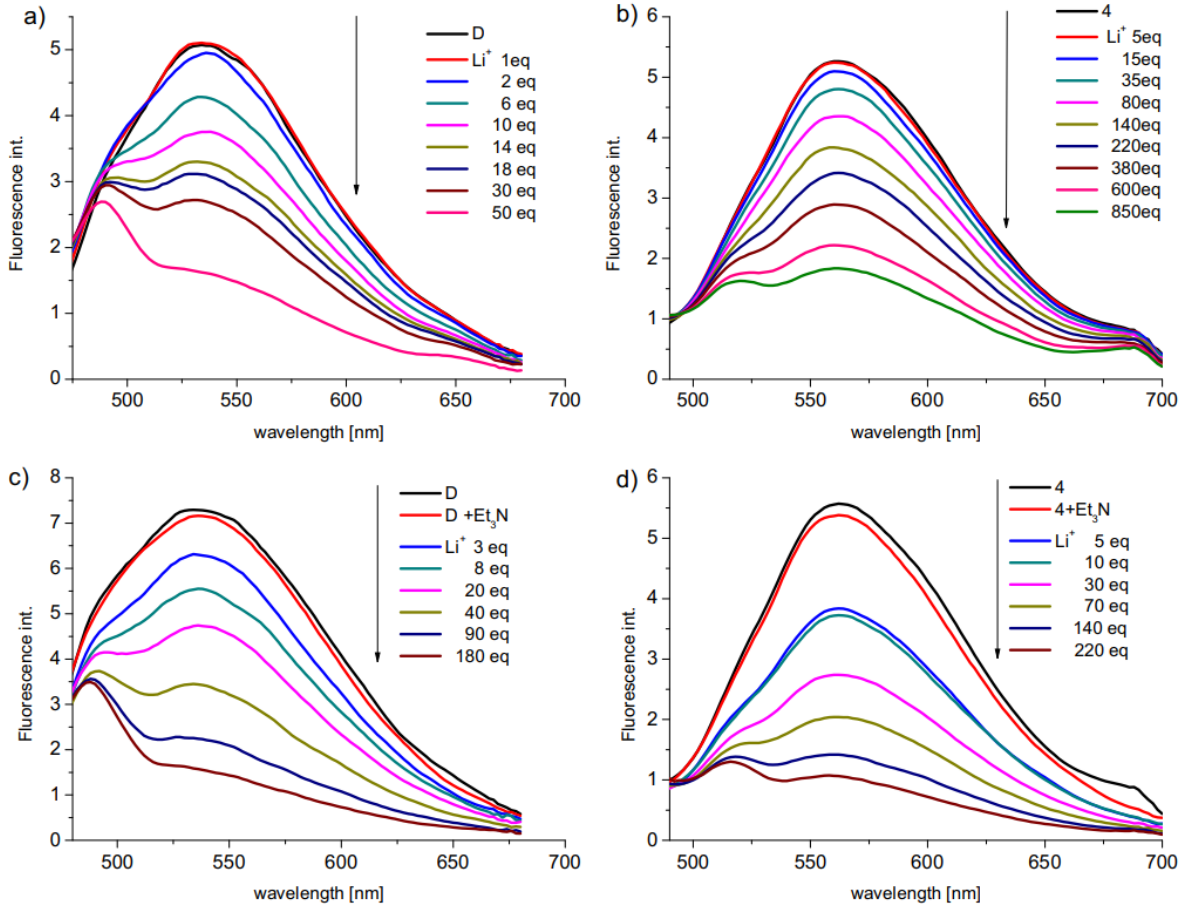

Fig. 12. Comparison of spectral changes upon titration with lithium perchlorate of a) **D** (3.0×10^{-5} M, λ_{ex} = 432 nm, λ_{em} = 452 nm) (lithium salt concentration: 0-1.28×10^{-3} M) in pure acetonitrile; b) **4** (1.1×10^{-5} M, λ_{ex} = 450 nm, λ_{em} = 580 nm) (lithium salt concentration: 0-5.14×10^{-3} M) in pure acetonitrile; c) **D** (1.9×10^{-5} M, λ_{ex} = 432 nm, λ_{em} = 452 nm) (lithium salt concentration: 0-2.60×10^{-3} M) in basic acetonitrile (pH ~10.5); d) **4** (1.1×10^{-5} M, λ_{ex} = 450 nm, λ_{em} = 580 nm) (lithium salt concentration: 0-1.90×10^{-3} M) in basic acetonitrile (pH ~10.5)

For comparison with results obtained from UV–vis titrations stability constant values (logK) of complexes of crowns **D** and **4** with lithium and sodium ions were also evaluated from fluorescence experiments. The obtained values are collected in Fig. 14. As it can be seen the trend in the strength of binding of metal cation is similar both in the ground and excited state. In both cases higher values for complexes of **4** – macrocycle bearing two phenyl residues as substituents in benzene rings were determined. Only in case of sodium ions similar logK values for **4** and **D** were found in the excited state.

https://doi.org/10.1016/j.jphotochem.2016.10.028

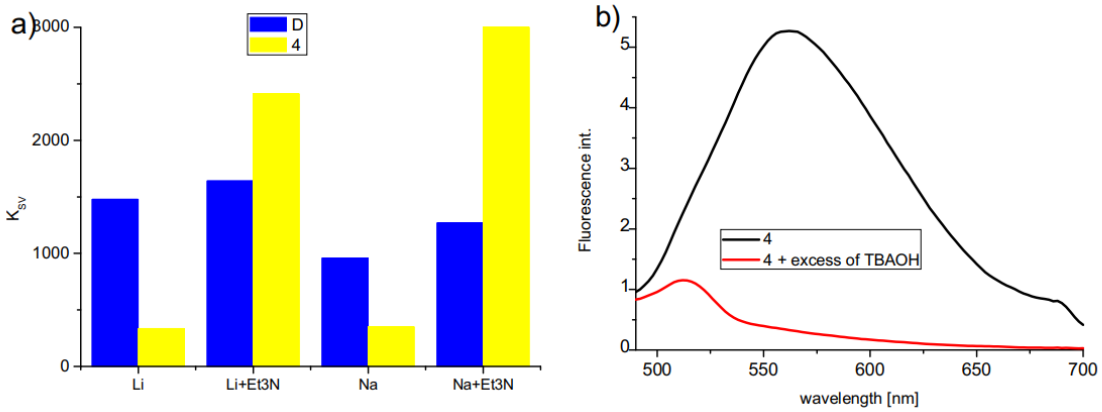

Fig. 13. Comparison of Stern-Volmer constant values for 16-membered diphenyl-hydroxyazobenzocrowns **D** and **4** and b) comparison of fluorescence spectrum of **4** and its spectrum registered in the presence of excess of tetra-*n*-butylammonium hydroxide.

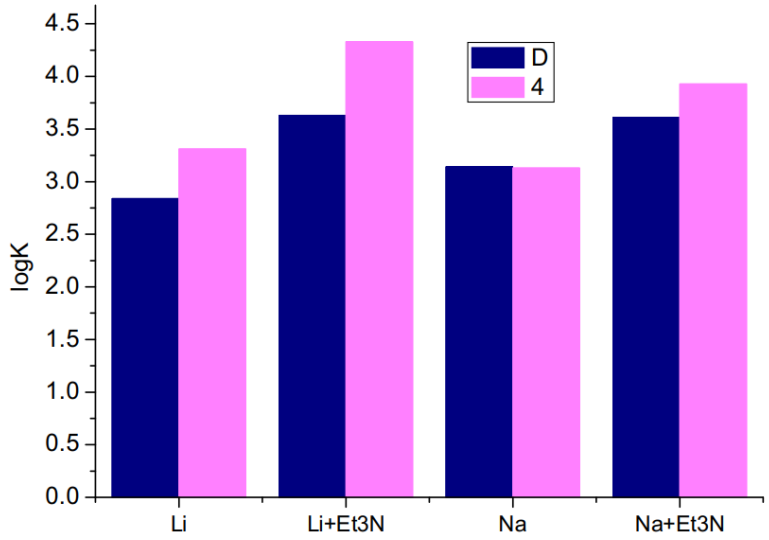

Fig. 14. Comparison of stability constant values of complexes of **D** and **4** with lithium and sodium cations evaluated from spectrofluorimetric experiments in pure and basic acetonitrile.

2.3. Protonation of diphenyl-azobenzocrowns

Azocompounds – weak bases – are protonated at one of two azo N-atoms forming non-symmetric π-complex [21]. Recently, we have shown that tautomeric equilibrium of hydroxyazocrowns is pH dependent [6h].

Here, having in mind the influence of phenyl moieties on metal cation binding strength, we find interesting to compare proton binding properties of previously described 13-membered crowns **A** and **C**, 16-membered **B** and **D** with their diphenyl analogs **1–4**. Spectral changes in the presence of *p*-toluenesulfonic acid are exemplified with results of titration experiments conducted for diphenyl crowns **1** and **4**. The titration of **1** with *p*-toluenesulfonic acid results in significant spectral changes: the absorption band at 360 nm is shifted towards 390 nm and a new band at 540 nm appears (Fig. 15a). Isosbestic point in this case is not sharp. It suggests more complicated system under equilibrium than only **1** and its protonated form. It cannot be excluded that *Z-E* isomerization of azobenzocrown under measurement conditions might be considered. The protonation of crown, similarly to described previously functionalized azobenzocrowns [12a], causes remarkable color change from yellow to red. Similar changes of absorption spectra (Fig. 15b) and color change to pink-red are observed for 16-membered diphenyl hydroxyazobenzocrown what

https://doi.org/10.1016/j.jphotochem.2016.10.028

is manifested by the appearance of new absorption band at 550 nm. Proton binding constants for diphenyl-azobenzocrowns **1–4** were estimated from titration experiments and compared with results obtained for compounds **A–D** (Fig.15c). Proton binding values are generally higher for hydroxyazobenzocrowns than for non-functionalized compounds. But among hydroxyazobenzocrowns protonation constant values are higher for macrocycles without phenyl rings as substituents.

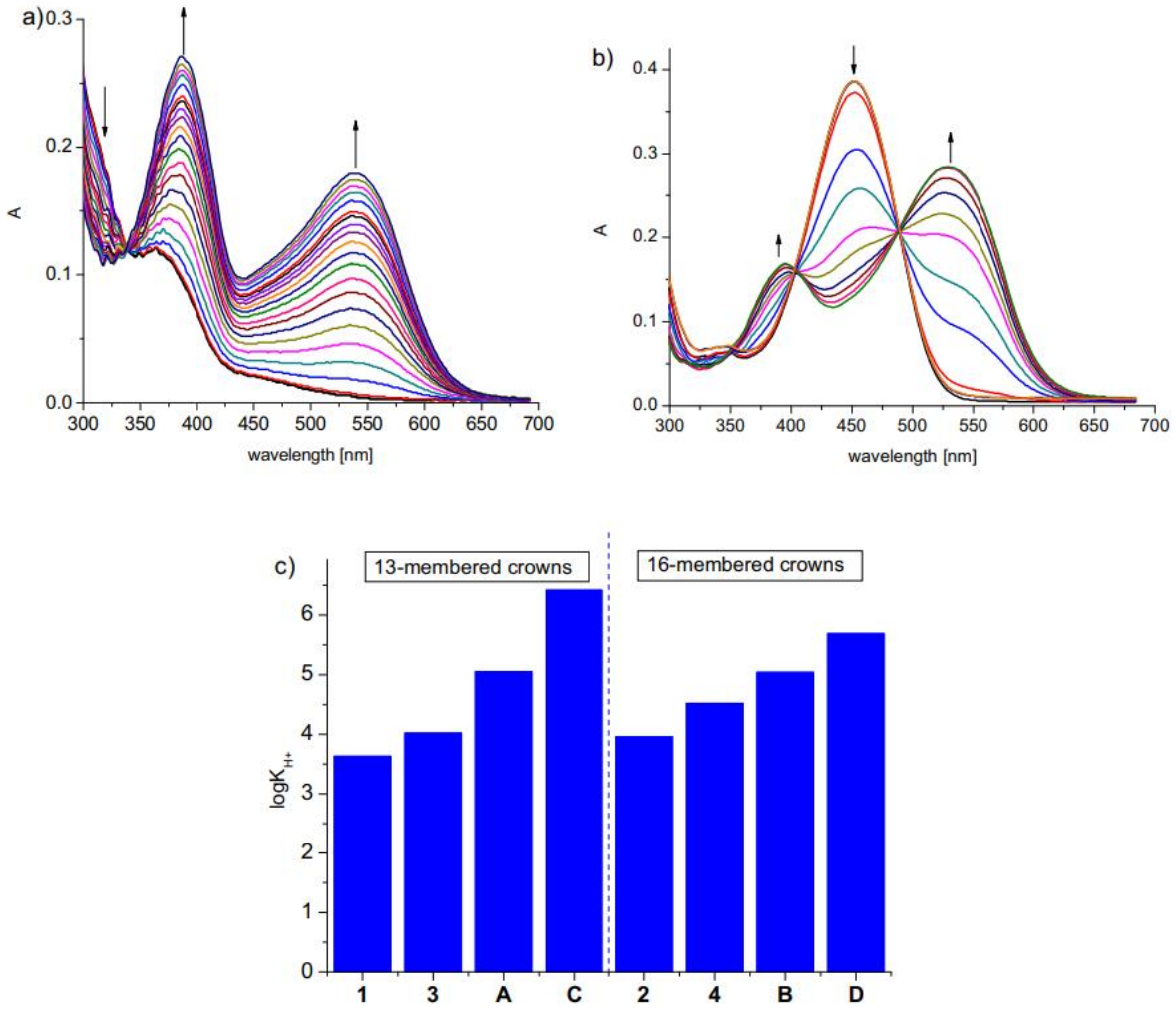

Fig 15. a) Changes in UV-vis spectrum of: a) **1** (2.4 × 10^{-5} M) upon titration with *p*-toluenesulfonic acid (0-3.2 × 10^{-4} M); b) **4** (7.9 × 10^{-6} M) upon titration with *p*-toluenesulfonic acid (0-1.9 × 10^{-4} M) in acetonitrile; c) comparison of proton binding constants for 13-membered (**1**, **3**, **A**, **C**) and 16-membered (**2, 4, B, D**) azobenzocrowns in acetonitrile.

2.4. X-Ray structure of 3

X-Ray structure of **3** shows that azobenzocrown crystallizes in quinone-hydrazone form. Molecular structure of **3** is shown in Fig. 16. Details characterized of X-ray structure are included in Supplementary data.

Bond length between nitrogen atoms is 1.338(14) Å, which is characteristic for a single bond. It is even longer than 1.317 Å noted previously for analogous crown with a -NH-N = group - compound **C** [22]. Much shorter bond 1.234 Å was found in azocrown with OH group in *meta* position to azo moiety [22] and isomers of **A**: 1.228 Å in *Z* isomer [6a], and 1.149 and 1.190 Å in *E* isomers [23]. Accordingly, C1-N1 bond is shorter than C13-N2 by ca 0.07 Å, which reflects its formally double bonding character. Atom O4 is attached to the C1-C6 ring and, may be a part of hydroxyl group or carbonyl group. No significant residual electron density is observed in the Fourier map close to O4. Taking

https://doi.org/10.1016/j.jphotochem.2016.10.028

into account the rather short C4-O4 bond length (ca 1.25 Å) and lack of hydrogen bond acceptors in the vicinity of O4, the presence of a carbonyl group (not a hydroxyl group) in the solid state must be assumed. All the described above features point to the presence of the quinone-phenylhydrazone tautomer in the solid state [22]. Actually four hydrogen bond donors of CH type and (internal H12 and intermolecular H3, H25a, H23b) are proximate to O4, see Fig. 17. Hydrogen bond donor inside the macrocycle cavity may be regarded as bifurcating to O1 and O3, although N2-H2···O1 geometry is more favorable, even if distances N2···O1 and N2···O3 are similar. Details for hydrogen bonding are gathered in Table S3 (Supplementary data).

Both nitrogen atoms and two of the oxygen ether atoms of the macrocycle lay almost in one plane, while the third O-atom O2 is shifted above the mean plane. Terminal phenyl rings are twisted relative to the rings to which they are attached to, so delocalization of electrons is not extended over all the benzene moieties. Dihedral angles between mean planes [24] are: ∠(C1–C6 and C7–C12) = 34.08°, ∠(C13–C18 and C19–C24) = 32.81°.

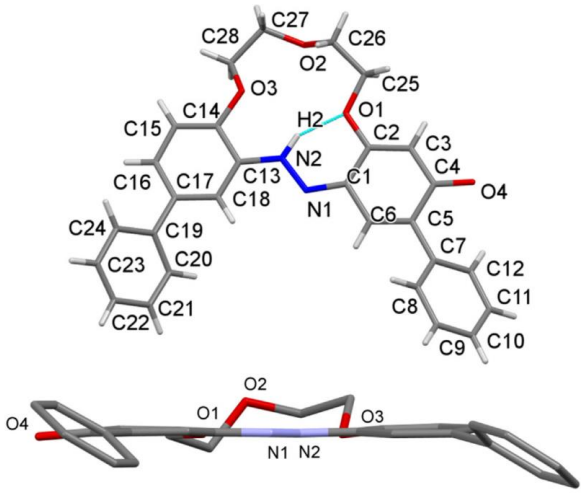

Fig. 16. Top: molecular structure and labeling for **3**; bottom: view of **3** along the mean plane defined by the azobenzene moiety.

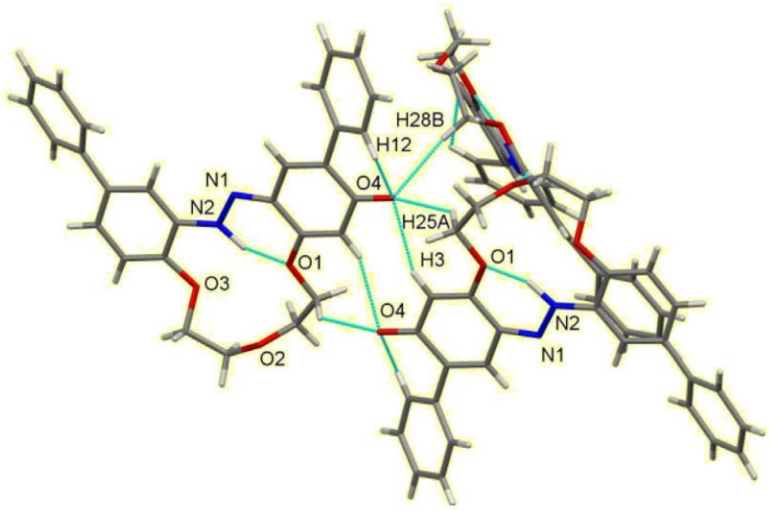

Fig. 17. Surroundings of O4 atom, indicating location of H-bonding donors and its C=O character.

3. Conclusions

Metal cation complexation studies for diphenyl-derivatives of 13- and 16-membered azobenzocrowns (compounds **1** and **2**) in acetonitrile were described for the first time. It was found that the presence of phenyl moieties in benzene rings affects the binding strength of metal cation and protonation of azobenzocrowns. The obtained values of stability constants differ for compounds without phenyl residues in benzene rings in para position to polyether linkage. For 13-membered

https://doi.org/10.1016/j.jphotochem.2016.10.028

diphenyl-azobenzocrown **1** stability constant of lithium complex is lower than for parent compound **A**. For larger 16-membered crown **2**, the stability constant values of complexes with alkali metal cations are comparable with parent crown **B** (except of potassium for which no spectral changes were observed in UV–vis spectra of **2**). In the case of alkaline earth metal cations the upward trend in binding constant values was observed according to increasing diameter of investigated ion. The highest value was found for barium complex. UV–vis and fluorescence measurements showed high complexation selectivity of diphenyl-hydroxyazobenzocrown **3** towards lithium (with stability constant value slightly lower than that of compound **C**) over sodium cation in basic (Et_3N) acetonitrile. Presence of phenyl moieties in benzene rings of 16-membered hydroxyazobenzocrown **4** influences both tautomeric equilibrium and metal cation binding affinity. Fluorescence was used for the first time for studies of metal cation complexation by hydroxyazobenzocrowns. Our measurements confirmed that metal cations in basic acetonitrile are complexed by ionized quinonehydrazone tautomers of hydroxyazobenzocrowns.

It was shown that diphenyl macrocycles **1** and **2** can be successfully used as ionophores not only in classic ISEs but also in miniature, all-solid-state type sensors. For the latter even better results were obtained (compound **1** as ionophore, sodium selective ISE) than for classic electrodes and ChemFETs.

The X-ray structure of 13-membered diphenyl-hydroxyazobenzocrown **3** was solved showing that in a solid state this compound exists in quinone-hydrazone form.

4. Experimental

4.1. General remarks

All chemicals of the highest available purity were purchased from commercial sources and used without further purification.

UV–vis spectroscopy (Unicam UV-300 spectrometer) was performed in acetonitrile. Fluorescence spectra were recorded on luminescence spectrometer (AMINCO Bowman Series 2 spectrofluorimeter) using flash xenon lamp. Bandpass of excitation and emission monochromators was 16 nm. Fluorescence spectra are uncorrected to instrument response. All emission spectra were recorded three times and averaged. For all measurements 1 cm quartz cuvettes were used and acetonitrile (LiChrosolv®) of gradient grade was used as a solvent. All salts, purchased from commercial sources, used in spectroscopic measurements were dried under vacuum at room temperature before use. ^{1}H NMR spectra were recorded on Varian instrument at 500 MHz. Chemical shifts are reported as δ [ppm] values in relation to TMS.

The screen-printed graphite electrodes were prepared in Institute of Electronic Materials Technology, Warsaw (plates of 18–15 mm with six electrodes, openings area ca. 1 mm^2). EMF measurements were carried out using 16-channel potentiometer a LAWSON LAB Inc. (USA). Deionized water (18 MΩ cm, Hydrolab, Poland) for EMF measurements was used.

4.2. Synthesis

Reductive macrocyclization of dinitropodands was used as a method of synthesis of diphenyl-azobenzocrowns **1** [8] and **2** [6] [6c]. Hydroxyazobenzocrowns **3** and **4** were obtained by the rearrangement of the respective azoxybenzocrown [12][12b]. Reference compounds **A–D** were synthesized according to previously described procedures [6a,g,h]. The characteristic features (TLC, mp, ^{1}H NMR, FTIR) of the final macrocyclic compounds are in agreement with the properties of the genuine samples of azobenzocrowns obtained and characterized by us previously.

https://doi.org/10.1016/j.jphotochem.2016.10.028

4.3. UV-vis and fluorescence experiments

4.3.1. Metal cation complexation

Complexation studies were performed by UV–vis titration of the ligand solution in acetonitrile with the respective metal perchlorates (for metal cations). *Caution! Perchlorate salts should be regarded as potentially explosive and handled with care.* The stock solutions of azobenzocrowns (~10^{-4} M) and metal perchlorates or TBA salt (~10^{-2} M) were prepared by weighing the respective quantities of them and dissolving in acetonitrile in volumetric flasks. Titrations of azobenzocrown solutions (2.3 mL) with metal perchlorates were carried out in a quartz cuvettes with path length of 1 cm. The stability constant values from UV–vis experiments were calculated with the use of OPIUM program titration data [25]. For evaluation of binding constant K from fluorescence measurements the following equation was applied:

$$F_0/(F - F_0) = [a/(b - a)][1/K[M] + 1]$$

Stability constant was determined as intercept/slope ratio from a plot $F_0/(F-F_0)$ versus $[M]^{-1}$. F_0 is fluorescence intensity of hydroxyazobenzocrown, F – fluorescence intensity in the presence lithium perchlorate, [M] – lithium perchlorate concentration.

Stern-Volmer constants K_{sv} [26] were determined graphically according to equation:

$$F_0/F = 1 + K_{SV}[Q]$$

where F_0 is fluorescence intensity in the absence of quencher, F – fluorescence intensity in the presence of quencher, [Q] – quencher metal perchlorate, triethylamine, TBAOH or $TBAClO_4$] concentration [M].

4.3.2. Protonation constants determination

The stock solutions, for working solutions preparation, of the crowns (~10^{-4} M) and *p*-toluenesulfonic acid (~10^{-2} M) were prepared by weighing the respective quantities of substances and dissolving them in volumetric flasks in acetonitrile. Azobenzocrowns working solutions (2.3 mL) were titrated with solution of *p*-toluenesulfonic acid. The protonation constant values were estimated from titration data with the use of OPIUM [25] program.

4.4. Ion-selective electrodes

Ca. 0.05 mg of carbon nanotubes (Thin MWCNT 95%, NANOCYL S.A., Belgium) in 1.2 mL of THF (freshly distilled over $LiAlH_4$) were sonicated for 1 h. Next, the remaining membrane constituents were added: 5 mg of ionophore (compound **1** or **2**), 50 mg of PVC, 0.1 mL of *o*-nitrophenyl-octyl ether (*o*-NPOE) and 1 mg of potassium *tetrakis*(4-chlorophenyl)borate. The solution (1 mL) (twice with an interval of 5 min) was applied onto graphite screen-printed electrodes, and the electrodes were left to dry over 24 h at room temperature. Next the electrodes were conditioned by soaking in a solution of NaCl or KCl (10^{-3} M), for sodium and potassium selective electrodes, respectively, for 10 h. A double-junction Ag/AgCl, KCl (1 M) reference electrode (Monokrystaly RAE 112) was used with 1 M NH_4NO_3 solution in the bridge cell. The selectivity coefficients were determined using the separate solution method (SSM) [10] at ion activities of 10^{-1} M.

4.5. X-ray crystal structure determination

Single crystals of **3** suitable for X-ray analysis were obtained by dissolving compound **3** in acetone. Acetone solution was left for slow evaporation of the solvent at room temperature.

X-ray diffraction measurements were carried out with a KM4 diffractometer (Kuma Diffraction, Wroclaw, Poland) with CCD detector (Oxford Diffraction, Yarnton, United Kingdom) using graphite monochromated MoKα radiation at 120 K. The temperature was stabilized by Oxford Cryosystems

https://doi.org/10.1016/j.jphotochem.2016.10.028

open flow nitrogen gas cooling device. Data collection and reduction was performed using [27]. The structure was solved by direct methods and refined anisotropically using the program packages WinGX 2013.3 [28] and SHELX-2013 [29]. Positions of the hydrogen atoms were calculated geometrically (except of the NH group) and taken into account with isotropic temperature factors. Generally hydrogen atoms were refined as raiding on their parent carbon atoms with usual constraints. The hydrogen atom H2 (linked to N2 atom) was found in the Fourier electron density map and refined with N-H bond length constrained to 0.88 Å.

Collection of diffraction data was technically difficult due to low diffraction power of the crystals. The best specimen selected required frame exposure time to be set as long as 280 s, which we assumed as our practical limit, still giving high R_{int} data quality parameter. After several days the data were affected by ice-formation so data set is only ca 60%. Nevertheless, the obtained electron density map is interpretable, so we decided to include the data to the paper.

Acknowledgements

Authors acknowledged support from sources for science GUT Grant No. 031402T004.

Authors thank anonymous reviewers for careful review, which helped us to improve the quality of above manuscript.

References

[1] **(a)** C. Renner, U. Kusebauch, M. Löweneck, A.G. Milbradt, L. Moroder, J. Pept. Res. 65 (2005) 4–14; **(b)** H. Nishihara, K. Kanaizuka, Y. Nishimori, Y. Yamanoi, Coord. Chem. Rev. 251 (2007) 2674–2687; **(c)** T.K. Tam, M. Ornatska, M. Pita, S. Minko, E. Katz, J. Phys. Chem C 112 (2008) 8438–8445; **(d)** F. Ercole, T.P. Davis, R.A. Evans, Polym. Chem. 1 (2010) 37–54; **(e)** A.A. Beharry, O. Sadovski, G.A. Woolley, J. Am. Chem. Soc 133 (2011) 19684– 19687; **(f)** R. Ahmed, A. Priimagi, Ch. F.J. Faul, I. Manners, Adv. Mater. 24 (2012) 926– 931; **(g)** Z. Li, J. Liang, W. Xue, G. Liu, S.H. Liu, J. Yin, Supramol. Chem. 26 (2014) 54– 65.

[2] L. Antonov (Ed.), Tautomerism: Methods and Theories, Wiley-VCH Verlag GmbH & Co. KGaA, 2013.

[3] **(a)** L. Antonov (Ed.), Tautomersim: Concepts and Applications in Science and Technology, Wiley-VCH Verlag GmbH & Co., 2016; **(b)** D. Debnath, S. Roy, B.H. Li, C.H. Lin, T.K. Misra, Spectrochim. Acta A: Mol. Biomol. Spectrosc 140 (2015) 185–197; **(c)** A. Mohammadi, H. Ghafoori, B. Ghalami-Choobar, R. Rohinejad, J. Mol Liq. 198 (2013) 44–50; **(d)** L. Antonov, V. Deneva, V. Kurteva, D. Nadeltcheva, A. Crochet, K.M. Fromm, RSC Adv. 3 (2013) 25410–25416.

[4] **(a)** M. Shiga, M. Takagi, K. Ueno, Chem. Lett. (1980) 1021–1022; **(b)** M. Shiga, H. Nakamura, M. Takagi, K. Ueno, Bull. Chem. Soc. Jpn. 57 (1984) 412–415; **(c)** R. Tahara, T. Morozumi, H. Nakamura, M. Shimomura, J. Phys. Chem. B 101 (1997) 7736–7743.

[5] E. Luboch, R. Bilewicz, M. Kowalczyk, E. Wagner-Wysiecka, J.F. Biernat, in: G. Gokel (Ed.), Azo Macrocyclic Compounds, in Advances in Supramolecular Chemistry, vol. 9, Cerberus Press, South Miami, USA, 2003, pp. 71–162.

[6] **(a)** J.F. Biernat, E. Luboch, A. Cygan, A. Yu. Simonov, A.A. Dvorkin, E. Muszalska, R. Bilewicz, Tetrahedron 48 (1992) 4399–4406; **(b)** E. Luboch, J.F. Biernat, E. Muszalska, R. Bilewicz, Supramol. Chem. 5 (1995) 201–210; **(c)** E. Luboch, J.F. Biernat, Y.A. Simonov, A.A. Dvorkin, Tetrahedron 54 (1998) 4977–4990; **(d)** E. Luboch, E. Wagner-Wysiecka, J.F. Biernat, J. Supramol, J. Supramol. Chem. 2 (2002) 279–291; **(e)** E. Luboch, E. Wagner-Wysiecka, Z. Poleska-Muchlado, V. Ch. Kravtsov, Tetrahedron 61 (2005) 10738–10747; **(f)** E. Luboch, E. Wagner-Wysiecka, T. Rzymowski, Tetrahedron 65 (2009) 10671–10678; **(g)** E. Luboch, Pol. J. Chem. 82 (2008) 1315–1318; **(h)** M. Szarmach, E. Wagner-Wysiecka, M.S. Fonari, E. Luboch, Tetrahedron 68 (2012) 507–515.

[7] D.G. Pijanowska, E. Luboch, J.F. Biernat, M. Dawgul, W. Torbicz, Sens. Actuators B: Chem. 58 (1999) 384–388.

https://doi.org/10.1016/j.jphotochem.2016.10.028

[8] Z. Mousavi, K. Granholm, T. Sokalski, A. Lewenstam, Sens. Actuators Chem. B 207 (2015) 895–899.
[9] A. Jasinski , M. Urbanowicz, M. Guzinski , M. Bochenska , Electroanalysis 27 (2015) 745–751.
[10] M. Han, Y. Norikane, Photoisomerization and light-driven fluorescence enhancement of azobenzene derivatives, in: A. Qin, B.Z. Tang (Eds.), Aggregation-Induced Emission: Fundamentals and Applications, John Willey & Sons, 2013, pp. 185–204.
[11] **(a)** P.S. Zacharias, S. Ameerunisha, S.R. Korupoju, J. Chem. Soc. Perkin Trans. 2 (1998) 2055–2060; **(b)** Y. Zhao, Q. Bo, Langmuir 23 (2007) 5746–5751; **(c)** M. Han, D. Ishikawa, E. Muto, M. Hara, J. Luminesc. 129 (2009) 1163–1168; **(d)** J. Yoshino, A. Furuta, T. Kambe, H. Itoi, N. Kano, T. Kawashima, Y. Ito, M. Asashima, Chem. Eur. J. 16 (2010) 5026–5035; **(e)** J. Nithyanandhan, N. Jayaraman, R. Davis, S. Das, Chem. Eur. J. 10 (2004) 689–698.
[12] **(a)** E. Wagner-Wysiecka, T. Rzymowski, M. Szarmach, M.S. Fonari, E. Luboch, Sens. Actuators B: Chem. 177 (2013) 913–923; **(b)** M. Szarmach, E. Wagner-Wysiecka, E. Luboch, Tetrahedron 69 (2013) 10893–10905.
[13] E. Wagner-Wysiecka, T. Rzymowski, M.S. Fonari, R. Kulmaczewski, E. Luboch, Tetrahedron 67 (2011) 1862–1872.
[14] H. Rau, Ber. Bunsen-Ges. Phys. Chem. 72 (1968) 637–643.
[15] **(a)** G. Gabor, Y. Frei, D. Geogiu, M. Kaganowitch, E. Fischer, Isr. J. Chem. 5 (1967) 193–211; **(b)** G. Geogiu, E. Fischer, Chem. Phys. Lett. 10 (1971) 99–101.
[16] H. Joshi, F.S. Kamounah, C. Gooijer, G. van der Zwan, L. Antonov, J. Photochem. Photobiol. A Chem. 152 (2002) 183–191.
[17] P. Nikolov, F. Fratev, S. Stoyanov, O.E. Polansky, Z. Naturforsch. 36a (1981) 191– 196.
[18] Y. Umezawa, P. Bühlmann, K. Umezawa, K. Tohda, S. Amemiya, Pure Appl. Chem. 72 (2000) 1851–2082.
[19] www.sigmaaldrich.com/catalog.
[20] L.M. Antonov, V.B. Kurteva, S.P. Simeonov, V.V. Deneva, Tetrahedron 66 (2010) 4292–4297.
[21] E. Haselbach, Helv. Chim. Acta 53 (1970) 1526–1543.
[22] E. Luboch, V. Ch. Kravtsov, J. Mol. Struct. 699 (2004) 9–15.
[23] M.S. Fonari, E. Luboch, A. Collas, A. Bukrej, F. Blockhuys, J.F. Biernat, J. Mol. Struct. 892 (2008) 195–199.
[24] A.L. Spek, Acta Cryst. D 65 (2009) 148–155 (PLATON).
[25] M. Kyvala, I. Lukeš, Program package “OPIUM” available (free of charge) at http://www.natur.cuni.cz/kyvala/opium.html.
[26] J.R. Lakowicz, Principles of Fluorescence Spectroscopy, 3rd edition, Springer Science+Business Media, New York, 2006.
[27] CrysAlisPro package CrysAlisPro, version 171: Agilent Technologies, Yarnton, England, 2011.
[28] L.J. Farrugia, J. Appl. Cryst. 45 (2012) 849–854.
[29] G.M. Sheldrick, Acta Cryst. A 64 (2008) 112–122.